International Symposium COMODIA 90: 263-268(1990)

Multi-Dimensional Modelling of Diesel Sprays Using a Fast Non-Iterative Implicit Solution Scheme – Recent Advances

A.P.Watkins and H.Khaleghi

Mechanical Engineering Department
University of Manchester
Institute of Science and Technology
Manchester M60 1QD
U.K.

ABSTRACT

This paper describes the main features and recent advances made in modelling sprays in real engines using a non-iterative but implicit solution scheme. The mathematical model together with the numerical procedure and solution algorithm employed are outlined briefly. The evaporation equations are modified in order to improve the prediction of evaporation rates of the droplets. The solution algorithm is modified to handle accurately the evaporation history of sprays with high evaporation rates. The effects of these changes on the results of simulations of flows in two engines are examined. In addition the flow results are examined to ascertain the effects of grid density and the treatment of the flow equations in the grid cell next to the injector hole.

INTRODUCTION

The authors and their colleagues have for several years been working on the development of computational fluid dynamics models for the calculation of multi-dimensional diesel sprays (1) - (4). The partial differential equations governing the gas phase are solved in Eulerian form by means of finite-volume techniques. The liquid spray phase equations are expressed in Lagrangian ordinary differential equations, and are solved by finite difference methods. The discrete droplet model used for the spray equations is based on that of O'Rourke and Bracco (5) and incorporates many of the recently proposed refinements, e.g. for droplet breakup (6).

Our code is, of course, not unique in incorporating these features. They appear also in the KIVA code (7) and the engine code due to Ramos (8). Where our code departs from these other codes, is the means by which the equations are solved. The KIVA code uses a semi-implicit solution methodology. Because of this, to maintain stability, the time steps which can be taken by the code are extremely small, usually around 0.5 μs for diesel spray calculations. This results in long computing times. The code of Ramos on the other hand uses iterative fully implicit methods. The implicit finite-difference equations allow any time step to be taken without the occurrence of instability. The only restriction on the time step is provided by the required accuracy of the results. Time steps many times larger than that of the KIVA code can be taken. However because the equations are solved iteratively the computation times can still be very long. In our code the equations are written in implicit form, but are solved using the non-iterative predictor-corrector method PISO (9), (10), (3). Experience has shown that computing times are reduced many times below those required for iterative solution.

Reference (1) and (2) presented early results obtained by the authors for sprays in realistic diesel engine geometries, namely a large, slow open-chamber quiescent-flow Mirrlees FV2 engine and a small high-speed engine equipped with an omega-shaped piston bowl, closely resembling a design by Fiat for automobile applications. Since that early work it has become apparent that a number of features of the modelling and coding needed amending.

The purpose of the paper is therefore two-fold. Firstly, to describe briefly the underlying methodology, in terms of the equations to be solved and the non-iterative implicit solution method employed for that purpose. Secondly to report on the amendments which have been made since 1987, and to present the latest results obtained.

MATHEMATICAL MODEL

The mathematical model employed to describe the motion and evaporation of liquid sprays in diesel engine is based on the discrete droplet formulation, which allows for gas-liquid interaction whilst solving for both the gas phase and the liquid phase.

For the gas phase the Eulerian conservation equations are solved of mass, momentum and energy together with the k-ϵ turbulence model. The presence of the liquid phase is accounted for by introducing the void fractions into these equations, and the vapour concentration is calculated by solving the fuel vapour mass fraction conservation equations. The general transport equation for flow in the cylinder of an internal combustion engine, with an expanding/contracting co-ordinate frame in the axial direction to account for the piston motion, takes the form:

$$\frac{1}{\Delta V}\frac{\partial}{\partial t}(\rho\theta\,\Delta V\,\varphi) + \nabla\cdot(\rho\theta\,\underline{V}_R\,\varphi) = \nabla\cdot(\Gamma_\varphi\,\theta\,\nabla\varphi) + \theta S_\varphi + S_\varphi^d \qquad (1)$$

Here φ represents any conserved property such as velocity components V_i, specific internal energy e_s, fuel vapour mass fraction f and turbulent quantities k and ϵ. ΔV is the local incremental volume, $\underline{V}_R$ is the relative velocity between the moving co-ordinate frame and the gas, ρ is the gas density and θ is the gas void fraction. Γ_φ and S_φ respectively represent the diffusion coefficients and associated gas phase source terms and are given fully in (3). The source term S_φ^d in general represents the mass, momentum and energy transfer between the liquid and gas phases.

The liquid phase is modelled as a spray of discrete droplet parcels which penetrate and interact with the gas phase. Each parcel contains many thousands of drops all having the same position, velocity, temperature, etc. The Lagrangian trajectory and momentum equations are solved to predict the position $\underline{\xi}_d$ and velocity $\underline{V}_d$ of the individual droplet parcels from:

$$\frac{d\underline{\xi}_d}{dt} = \underline{V}_d \qquad (2)$$

and

$$\frac{d\underline{V}_d}{dt} = K_d\ (\underline{V} + \underline{v}' - \underline{V}_d) + S_{\underline{V},d} \qquad (3)$$

where K_d is the drag function, $\underline{V}$ and $\underline{v}'$ are respectively the mean and fluctuating components of the gas velocity and $S_{\underline{V},d}$ represents source terms such as centrifugal and coriolis forces caused by any grid curvature. Full details of these equations are given in (3).

The equations describing the evaporation history of the droplets are expressed in a Lagrangian form as:

$$\frac{dm_d}{dt} = -\pi D_d D \frac{P_t}{R_f T_m} \ln\left[\frac{P_t}{P_t - P_{v,s}}\right] Sh \qquad (4)$$

and

$$m_d Cp_d \frac{dT_d}{dt} = \pi D_d K (T - T_d)\left[\frac{z}{e^z - 1}\right] Nu + Q \frac{dm_d}{dt} \qquad (5)$$

These equations (4) and (5) contain three unknowns, namely the droplet mass m_d, droplet temperature T_d and the local gas temperature T. A third equation is therefore required to close the equation set. This is provided by the truncated gas energy equation:

$$\frac{\partial}{\partial t}(\rho\theta\ C_v\ T) = -\frac{1}{\delta v}\frac{d}{dt}(m\ C_v\ T)_d \qquad (6)$$

in which it is assumed that the energy transfer between the phases is the dominant process compared with the convection and diffusion processes. In the above equations D_d is the droplet diameter, P_t is the total pressure, $P_{v,s}$ is the vapour pressure at droplet surface, T_m is the mean temperature, R_f is the fuel vapour gas constant and δv is part of the gas phase cell volume proportionally assigned to each droplet parcel. D and K are respectively the film diffusivity and thermal conductivity, C_p and C_v are the specific heats, Q is the latent heat of evaporation, Nu and Sh are Nusselt and Sherwood numbers respectively and z is a factor by which the heat transfer coefficient is corrected to account for simultaneous presence of mass transfer and is defined as:

$$z = \frac{Cp_v \frac{dm_d}{dt}}{\pi D_d K Nu} \qquad (7)$$

where Cp_v is the fuel vapour specific heat at constant pressure. These highly non-linear equations (4) - (7) are solved using the Newton-Raphson algorithm.

The equations governing the collision and coalescence (5) and secondary break up of the droplets (6) are included in the computer model. Drop collision and break up models are not activated in the present calculations but results obtained with break up and collision are extensively reported in (11).

NUMERICAL MODEL

The Eulerian gas phase conservation equations are transformed into solvable algebraic equations using finite volume techniques. The solution domain is divided into a number of discrete volumes and the finite volume equations are obtained by integrating the partial differential equations over the given control volume. The Euler implicit temporal differencing scheme and the hybrid scheme of upwind and central spatial differencing are used to discretise the equations. The droplet phase equations are discretised using the same temporal differencing as the gas phase, and the same time step.

The non-iterative Engine-PISO algorithm (3), (10) is employed to solve the finite difference equations in a three step predictor-corrector manner. In this algorithm at each time step, after the new droplets are introduced from the injector hole, the following calculations are made:

Firstly the position, velocity, diameter and temperature of all the droplets are predicted ($\underline{\xi}_d^*$, $\underline{V}_d^*$, D_d^* and T_d^*) by solving eqns. (2) - (7). Then, the new gas phase velocity components ($\underline{V}^*$) are predicted by solving the combined gas-liquid momentum equation using the prevailing density, velocity and pressure fields. Using these predicted values of droplet and gas quantities the droplet position, velocity, diameter and temperature are corrected for the first time ($\underline{\xi}_d^{**}$, $\underline{V}_d^{**}$, D_d^{**} and T_d^{**}), after which the first pressure correction equation is solved to correct the pressure field (p^*) and hence the gas velocity field ($\underline{V}^{**}$). Now, the final values of droplet position, velocity, diameter and temperature ($\underline{\xi}_d^{***}$, $\underline{V}_d^{***}$, D_d^{***} and T_d^{***}) are calculated followed by calculating the fuel vapour mass fraction field (f^*) and the gas energy field (e_s^*). The second gas phase pressure correction equation is solved to update the pressure field (p^{**}) and correct the velocity field ($\underline{V}^{***}$). Finally, the turbulent kinetic energy (k^*) and its dissipation rate (ϵ^*) are first predicted and then corrected to k^{**} and ϵ^{**} level through a point-by-point correction method. Full details of the algorithm and the equations are given in (3) and (10).

TEST CASES

Two test cases, namely the Fiat designed engine and the Mirrlees FV2 engine, have been chosen for this study. The Fiat engine whose shape is shown in Fig. 1 has a 72.8 mm bore, 100 mm stroke and 2.5 mm clearance. It is equipped with an omega-shaped piston bowl with an entrance radius of 26 mm. The engine speed is taken as 3500 rpm. The geometry of the Mirrlees engine is shown in Fig. 2.

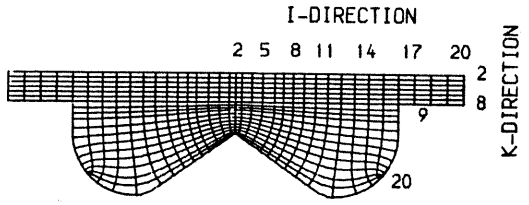

Fig. 1 Fiat designed engine - Shape and grid distribution

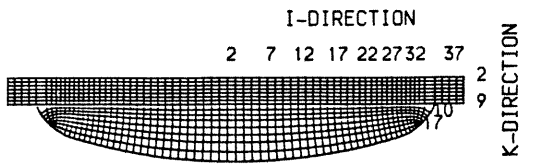

Fig. 2 Mirrlees FV2 engine - shape and grid distribution

This is a large four-stroke quiescent engine with 304.8 mm bore, 381 mm stroke, 9.3 mm clearance and 133.35 mm bowl radius. The engine speed is 500 rpm. Typical grid distributions are also illustrated in Figs. 1 and 2. The Fiat engine uses a four-hole injector nozzle of hole diameter 0.265 mm which directs the fuel into the bowl at an angle of 25° to the cylinder head, whereas in the Mirrlees engine a five hole injector of 0.7mm hole diameter is used with injection angle of 22° to the cylinder head. For both engines the flow calculations start at inlet valve closure by specifying the initial conditions and proceed in 1° crank angle steps. During the injection phase which starts at 17° BTDC in both engines the fuel spray from only one of the holes is calculated by assuming cyclic boundaries between the sectors. Calculations are stopped at 2° BTDC. The sizes of the droplets at nozzle exit are taken from a Rossin-Rammler distribution assuming a Sauter mean diameter.

RESULTS AND DISCUSSION

The Fiat Engine

This engine has been used as the main test case for the code. Injection starts at 17° BTDC when the pressure and temperature are 30 bar and 750 K respectively and proceeds up to 2° BTDC when combustion should be capable of taking place. Although no experimental data exist for this case, the latter condition does provide a means of analysing the results. By 2° BTDC fuel vapour mass fraction levels should exist within the flammability limits around the stoichiometric value of about 0.06. In the calculation which was originally made for this engine (2), using a 25 μm Sauter mean diameter, much lower fuel vapour concentrations than this (everywhere less then 0.03) were predicted. The total percentage of mass evaporated by 2° BTDC was only 2.6% of the total mass injected. This result is shown as Step 1 in Fig. 3. A thorough survey of the equations, particularly relating to fuel properties and evaporation showed that a number of modifications and corrections had to be made to the equations and the solution algorithm in order to obtain a realistic evaporation history. These are described below:

Negative evaporation was found to be present in the early stages of the injection period. It was found that the negative evaporation arises if the couplings between the droplet diameter, density and temperature as well as the gas temperature and other physical properties are not handled in an appropriate manner. In particular the rate of change of droplet density with droplet temperature had to be allowed for when solving equations (4) - (7). When these changes were made, the negative evaporation was eliminated and the final evaporation rose to 3.9%, shown in Fig. 3 as Step 2.

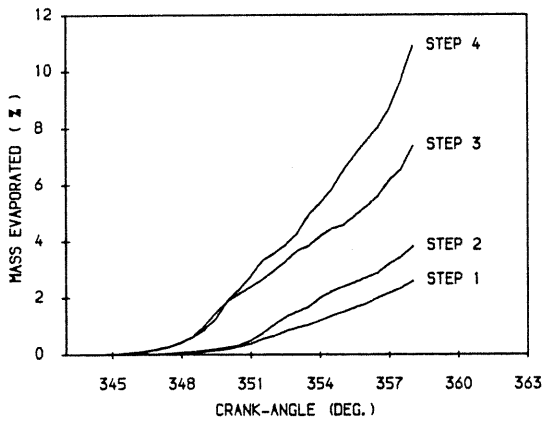

Fig. 3 Step-by-step improvement in evaporation rates - Fiat engine

Furthermore the total evaporation rose to about 7.5% when the gas constant R_f was assigned the value for the fuel vapour as suggested in (12) instead of that for the mixture of fuel vapour and air as previously used in the code (Step 3). More importantly a survey of the evaluation of the fuel vapour, air and mixture properties revealed that the fuel vapour mass fraction had not been consistently applied in a number of the equations; in particular in the evaluation of the mixture specific heat used in the overall energy equation and the mixture gas constant used in the equation of state. These corrections were supplemented by updating the gas temperature and density not only after calculating the new energy field but also after calculating the fuel vapour fraction field. Applying these corrections increased the total evaporation to about 11%, as shown in Fig. 3 as Step 4. The corresponding fuel vapour mass fraction field for Step 4 is shown in Fig. 4 where it is seen a maximum vapour concentration of 5% has been obtained by 2° BTDC compared with less than 3% in the original calculation.

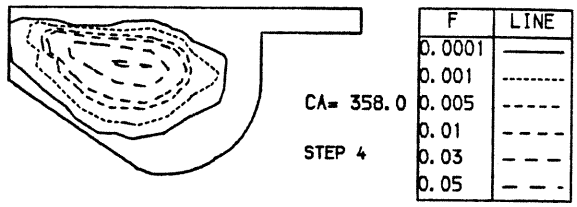

Fig. 4 Fuel vapour mass fraction contours near TDC - Step 4

Despite the significant improvements made in the level of evaporation the maximum value of fuel vapour mass fraction is still lower than the required stoichiometric value. This is most probably due to the relatively large initial Sauter mean diameter of 25 μm used in these calculations. Recourse was therefore necessary to the use of smaller drops, as used in the KIVA code (7) and the code of Ramos (8), to enhance evaporation. So calculations were made with Sauter mean diameters of 15 μm, 5 μm and 3 μm, representing a wide range of evaporation levels. This again revealed a number of weaknesses in the code, particularly for smaller Sauter mean diameter cases. Most importantly it became apparent that, due to the non-iterative nature of the solution methodology, it was crucial to solve in the correct order the gas phase equations relating to the evaporation of fuel, i.e. the fuel vapour mass fraction and the gas energy equation. This is because for sprays with high evaporation rates the fuel vapour mass fraction plays a dominant role in determining the evaporation process, so its solution should proceed that of the gas energy equation, if iteration is to be avoided.

Fig. 5 illustrates the evaporation rate from a spray with small drops obtained from alternative methods employed here. Method 0 is the original code before the corrections were made to the mixture specific heat and gas constant as described above. Although this method worked well for sprays with low rates of evaporation, it was found to be totally non-applicable for high evaporation rates. Method 1 incorporates all the amendments referred to so far. Method 2 solves the gas phase equations for fuel vapour concentration before the energy equations, rather than in the reverse order as is the case in Methods 0 and 1. Method 1 gives a final evaporation of about 30% compared with about 52% obtained from Method 2. As a check on which method is correct, Method 3 shows the results of iterating around these two sets of equations. This gives a final evaporation of about 40%. This lies between the results of Method 1 and 2, and the history of the evaporation is quite different. However, Fig. 6 shows that by halving the time step used, Method 2 gives very similar results to Method 3. The time step is then

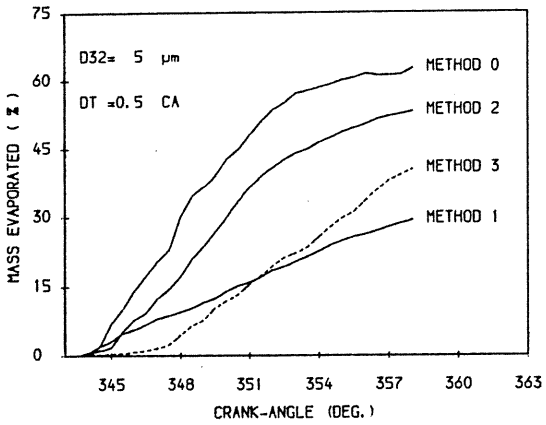

Fig. 5 Evaporation rates for small drops - comparison of solution methods

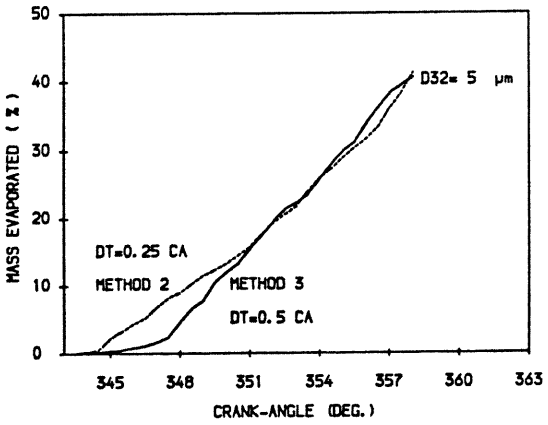

Fig. 6 Time step influence on evaporation rates - small drops

approximately 12 μs (0.25° crank angle), i.e. still many times larger than that permissible in the KIVA code. Method 2 would appear to give an accurate prediction of evaporation as long as the time step is short enough.

Fig. 7 shows the predicted fuel vapour mass fraction field obtained at 2° BTDC using Method 2 with time step equivalent to 0.25° crank angle. Clearly large parts of the vapour concentration now lie within the flammability limits. More details of these calculations are given in (4).

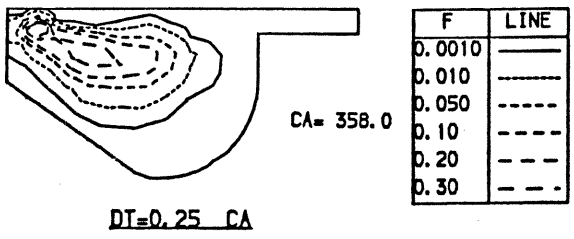

Fig. 7 Fuel vapour mass fraction contours near TDC - small drops

The effects of grid refinement on the spray and flow pattern have been examined using the Fiat engine. Five grids have been used ranging from Grid A (coarse, 12 x 6 x 12) to Grid E (fine, 38 x 14 x 22) to cover a quadrant of the engine. Grid C is the medium grid and contains 20 x 10 x 20 grid lines (see Fig. 1). The predicted spray structure and the gas flow field obtained from the coarse, medium and fine grids are shown in Fig. 8 at 2° BTDC and the effects of grid density on the penetration rate are shown in Fig. 9. It

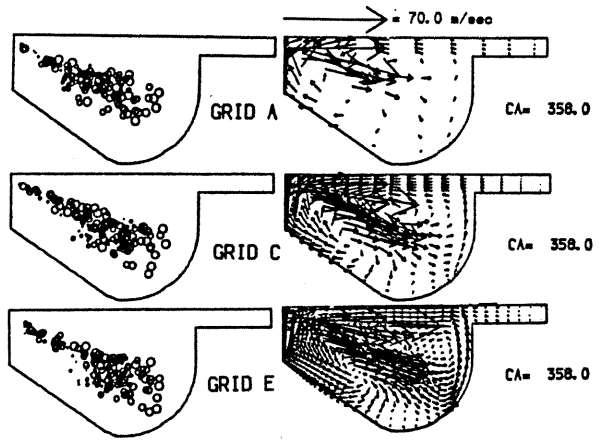

Fig. 8 Grid refinement effects on spray and flow field near TDC

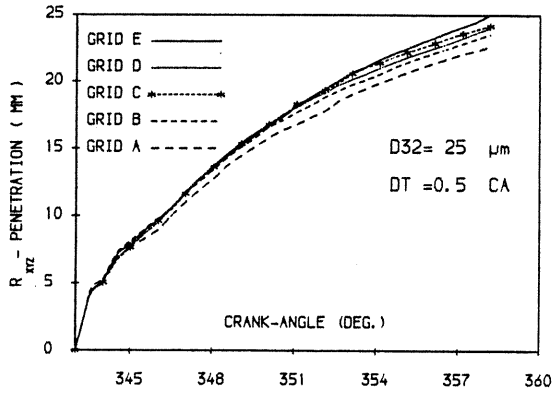

Fig. 9 Grid refinement effects on spray penetration

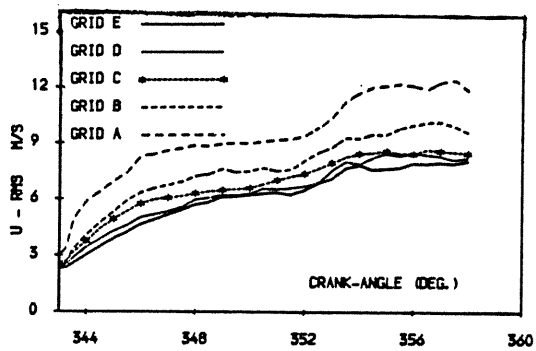

Fig. 10 Variation of average rms values of velocity with different grids

is seen from these figures that apparently all the main features of the spray and the flow are captured even by the coarsest grid. However the spray penetrates deeper into the bowl and the flow pattern is improved as the grid density is

increased. From the analysis of the spray results so far it can be seen that Grid C is an accurate and economical grid for the calculations. To prove this further, the average root mean square (RMS) values of all three velocity components were calculated for all the grids involved and plotted against time. As shown in Fig. 10, for the radial velocity component (U), the calculated U-RMS values for grids C, D and E remain almost the same throughout the calculation. RMS values of V and W (not shown here) are much closer. From this is deduced that Grid C is sufficiently fine to eliminate most truncation errors, for this case.

The Mirrlees Engine

Calculations were presented in (1) for this engine with the original code, using a very coarse grid (18 x 6 x 14), a 0.25° crank angle interval and a 25 μm Sauter mean diameter for the injected drops. In that paper too little fuel was evaporated by 2° BTDC (about 6%) and as shown in Fig. 11(a) the spray was deflected upward from its original direction. Figure 11(b) shows the spray pattern for the same conditions, but incorporating all the amendments described above. The evaporation rose to about 42% and the penetration dramatically reduced as a result.

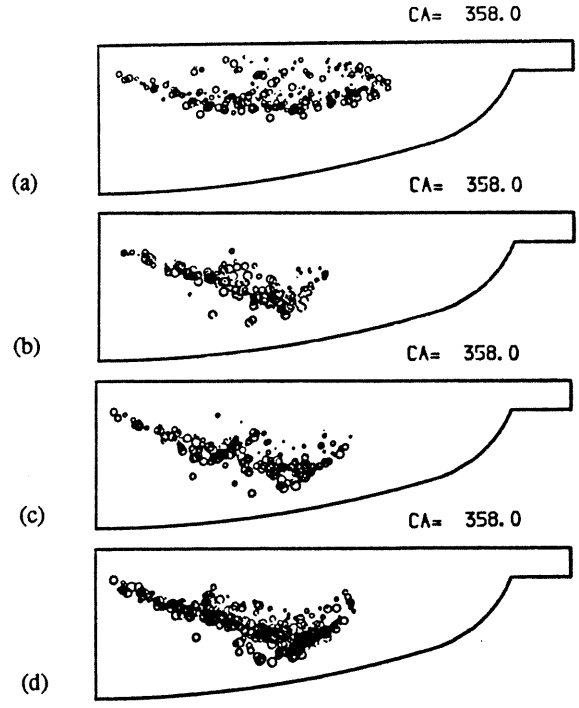

Fig. 11 Mirrlees engine - spray field near TDC
(a) original results (1)
(b) after amendments and using small drops
(c) amended injection cell-treatment
(d) time step halved from (c)

The present model assumes that the gas in the cell next to the exit of the injector (the injection cell) is accelerated to the same velocity as the liquid at the downstream face of the cell. This velocity is calculated from the momentum balance of the injection cell. Clearly if the gas mass is significant compared with the liquid mass this approach leads to a sharp reduction in the liquid velocity. It is therefore essential to keep the injection cell as small as possible. To eliminate the role of the injection cell size from the calculation the droplets were introduced into the chamber without transferring any momentum to the injection cell and the injection cell gas velocity was calculated from the gas momentum equation just as for all the other cells. As it seen from Fig. 11(c) the spray has penetrated by about 12% further into the bowl and the evaporation rose to about 50% as a result of this new treatment.

To calculate the evaporation more accurately the above calculations were redone with the time step reduced to 0.125° crank angle. As shown in Fig. 11(d) neither the spray structure nor the final penetration were significantly effected. The evaporation however was reduced to about 40%.

The grid used for the above calculations was too coarse to give a satisfactory level of truncation errors. To increase the numerical resolution and reduce the effects of numerical diffusion in this engine a finer grid of the size 37 x 14 x 17 (see Fig. 2) was required to cover a 72° sector of the cylinder. Fig. 12 illustrates the final results of the Mirrlees engine flow (spray structure, flow field and fuel vapour concentration) which is markedly different from that reported in (1). The spray here has penetrated deep into the bowl instead of being deflected upward, the flow field has correspondingly changed and peak values of fuel vapour mass fraction above 10% have been obtained here compared with about 1% in (1).

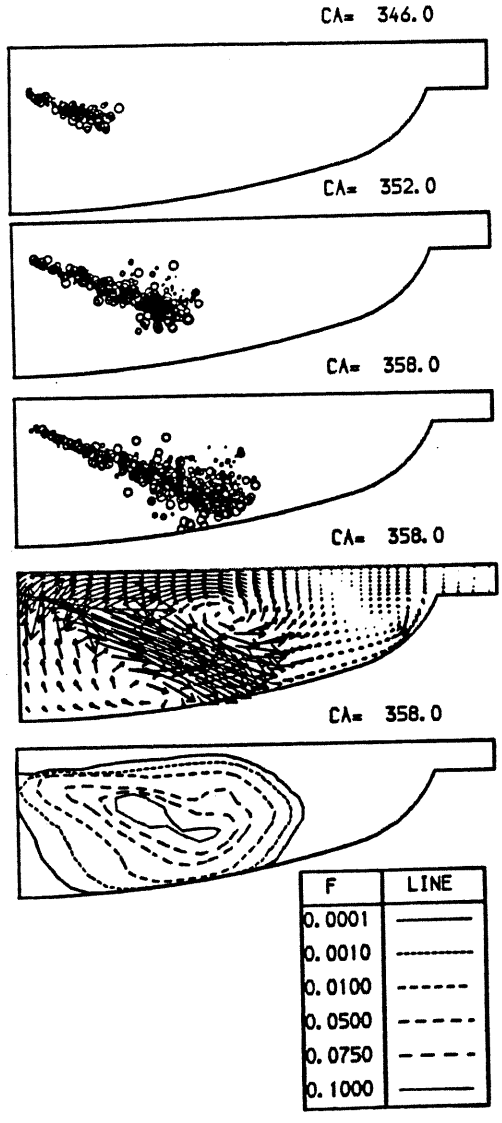

Fig. 12 Mirrlees engine - fine grid results

Further advances are described in other papers submitted to this symposium. In particular, a new model to account for the impaction of sprays on a wall is described by Watkins and Wang (13), and measures which can be taken to partially alleviate the effects of false diffusion on the spray are reported by the present authors (14).

CONCLUSIONS

This paper has reported on the recent advances made in the developments of the Engine-PISO spray code. The evaporation prediction of the model was significantly improved from those previously reported for both the Fiat and Mirrlees engines. This was made by rectifying a number of numerical and modelling errors previously present in the code. It was also shown that, if the non-iterative EPISO algorithm is to be employed when evaporation rates are high, the fuel vapour mass fraction equation must be solved before the gas phase energy equation and the time step must be kept reasonably short. However, the time step is still many times larger than for the KIVA code. The effect of grid dependency for both engines was examined and it was found that a much finer grid was required for the Mirrlees engine to minimise the truncation error. Changes in the treatment of the injection cell led to a 12% increase in the spray penetration in the Mirrlees engine.

Overall the results presented here are very different from those presented in earlier papers, due to the significant changes made in the modelling and the computer code.

REFERENCES

1. Watkins, A.P. and Khaleghi, H., "Three-dimensional diesel engine spray modelling", Paper No. C12/87, I.Mech.E. Conf. on Computers in Engine Technology, Cambridge, 1987.
2. Khaleghi, H. and Watkins, A.P., "Calculation of three-dimensional diesel sprays into curvilinear piston bowls", Paper No. 87-FE-1, ASME Symp. on Automotive Engine Technology, Dallas, 1987.
3. Watkins, A.P., "Three-dimensional modelling of gas flow and sprays in diesel engines", Computer Simulation of Fluid Flow, Heat and Mass Transfer and Combustion in Reciprocating Engines (Markatos, N.C. ed.), Hemisphere, pp. 193-237, 1989.
4. Watkins, A.P. and Khaleghi, H., "Modelling diesel spray evaporation using a non-iterative implicit solution scheme", Accepted for publication by Appl. Math. Modelling, 1990.
5. O'Rourke, P.J. and Bracco, F.V., "Modelling of drop interactions in thick sprays and a comparison with experiment", Proc. I.Mech.E. Conf. on Stratified Charge Automotive Engines, 1980.
6. Reitz, R.D. and Diwakar, R., "Structure of high-pressure fuel sprays", SAE Paper No. 870598, 1987.
7. Amsden, A.A., Butler, T.D., O'Rourke, P.J. and Ramshaw, J.D., "KIVA - a comprehensive model for 2-D and 3-D engine simulations", SAE paper No. 850554, 1985.
8. Ramos, J.I., "Modelling heat and mass transfer in diesel engines: from thermodynamic models to multidimensional calculations", Computer Simulation of Fluid Flow, Heat and Mass Transfer, and Combustion in Reciprocating Engines (Markatos, N.C. ed.), Hemisphere, 1989.
9. Issa, R.I., "Solution of the implicitly discretised fluid flow equations by operator splitting", J. Comput. Phys., Vol. 62, No. 1, pp. 40-65, 1986.
10. Ahmadi-Befrui, B., Gosman, A.D., Issa, R.I. and Watkins, A.P., "EPISO - an implicit non-iterative solution procedure for the calculation of flows in reciprocating engine chambers", Comp. Meth. Appld. Mech. Engrg. (in press), 1990.
11. Khaleghi, H., "Three-dimensional modelling and comparison with experiment of sprays and gas flow in test rigs and diesel engines" PhD Thesis, University of Manchester, Faculty of Technology, 1990.
12. Borman, G.L., and Johnson, J.H., "Unsteady vaporisation histories and trajectories of fuel drops injected into swirling air", SAE paper No. 598C, 1962.
13. Watkins, A.P. and Wang, D.M., "A new model for diesel spray impaction on walls and comparison with experiment", Int. Symp on Diagnostics and Modelling of Combustion in Internal Combustion Engines, Kyoto, 1990.
14. Watkins, A.P., and Khaleghi, H., "An ad-hoc procedure to alleviate false diffusion effects in computer codes using discrete droplet models", Int. Symp. on Diagnostics and Modelling of Combustion in Internal Combustion Engines, Kyoto, 1990